

1 **DEEP LEARNING-BASED APPROACH FOR URBAN DRIVEWAY IDENTIFICATION**
2 **FROM AERIAL IMAGERY**

3

4

5

6 **M M Mahabubur Rahman**

7 Computer Science, Texas State University
8 601 University Dr, San Marcos, TX 78666
9 Email: toufik@txstate.edu

10

11 **Subasish Das**

12 Civil Engineering, Texas State University
13 601 University Dr, San Marcos, TX 78666
14 Email: subasish@txstate.edu

15

16 **Jelena Tešić**

17 Computer Science, Texas State University
18 601 University Dr, San Marcos, TX 78666
19 Email: jtesic@txstate.edu

20

21

22 Word Count: 5287 words + 4 table(s) × 250 = 6287 words

23

24

25

26

27

28

29 Submission Date: October 7, 2023

1 ABSTRACT

2 Roadways facilitate drivers' mobility and provide access to land development and commercial es-
3 tablishments. However, conflicts can arise when roadways are expected to cater to high-speed
4 traffic and simultaneously offer direct entry to properties. Access management becomes critical
5 in such scenarios, necessitating careful planning and comparison crucial to arterial and collec-
6 tor roadway systems. Access points are paramount in connecting public roadways with adjacent
7 properties; they also contribute significantly to traffic accidents and congestion. To address these
8 challenges, access management initiatives focus on specific corridors. Strategic approaches uti-
9 lizing geographic information systems (GIS) can aid the decision-making process efficiently and
10 effectively. This research introduces a comprehensive framework for detecting and classifying
11 driveway density in a given location. The proposed framework utilizes Open Street Map (OSM)
12 road network data to identify the coordinates of access points and corresponding Google Map
13 satellite images for these points. A pre-trained Deep Neural Network (DNN) model is employed
14 to extract deep features from the satellite images, and the k-Nearest Neighbor (k-NN) search is
15 applied to classify the access points. The framework achieves an accuracy of 54.48%, surpassing
16 the conventional DNN model by 0.35%, based on experimental Austin satellite image data. This
17 framework aims to enhance access management strategies and improve road safety by harnessing
18 advanced technologies and geospatial data.

19

20 *Keywords:* Driveway densities, Computer vision, Safety performance.

1 INTRODUCTION

2 Roadways serve two primary purposes: meeting the mobility requirements of drivers and granting
3 direct entry to land development, including commercial establishments. Certain types of roadways
4 are functionally categorized, designed, and regulated to cater to the needs of high-speed traffic
5 passing through. A relevant example of such roadways is the Interstate Highway System in the
6 United States, which lacks provisions for direct land access. Conversely, most roadways worldwide
7 consist of local urban streets or rural roads. These roadways are primarily intended to facilitate
8 limited traffic and predominantly offer low-speed access to neighboring and nearby properties.

9 Conflicts related to access arise when the primary purpose of a roadway becomes ambigu-
10 ous. Most access-related conflicts occur on routes expected to serve through traffic and provide
11 property entry. Typically, these problematic routes are categorized as arterial or collector based
12 on their function (1). Access management involves careful planning and controlling direct entry
13 points from land development (whether through the public roadway system or private driveways) to
14 the arterial and collector roadway systems. This is achieved through various measures and guide-
15 lines, including standards for driveway spacing, clearance at driveway corners, the implementation
16 of alternative access routes like frontage roads, and the installation of raised medians.

17 Access points are crucial in the road transportation network as they connect public road-
18 ways, adjacent properties, private developments, and facilities. However, access points also signif-
19 icantly contribute to traffic crashes and congestion (2–4). Their positioning, design, and visibility
20 often fail to meet the necessary safety standards for both vehicles and pedestrians. The left-turn
21 movements, both entering and exiting the access points, are a significant factor in their inadequate
22 safety performance. A comprehensive study on driveway crashes categorized by maneuver and
23 collision type revealed that over 65% of accidents involving driveways occurred when vehicles
24 were turning left into the access point (5). Research indicates that approximately 5% of urban
25 crashes can be directly attributed to the presence of access points, while in rural areas, this per-
26 centage rises to 7% (6, 7). Adding one access point per mile on two-lane roads in both urban and
27 rural settings leads to an increase in the crash rate of approximately 1.5% (8, 9). Furthermore, sev-
28 eral studies have found a relationship between the crash rate and the square root of access density
29 (2, 10). Moreover, the Highway Safety Manual (HSM) (11) requires the inclusion of driveway den-
30 sities based on land use type to develop safety performance functions (SPFs) for specific roadway
31 facilities. For instance, urban access points are categorized into seven types: Major residential,
32 Minor residential, Major industrial, Minor industrial, Major commercial, Major commercial, and
33 other (11). As this data is not readily available, researchers use multiple approaches (including a
34 manual count of driveways, which is labor intensive) to address this information gap.

35 Access management initiatives are typically planned and executed on a corridor-specific
36 basis (12). However, it is also possible to adopt more strategic approaches to access management
37 by leveraging technologies like geographic information systems (GIS). These advanced tools en-
38 able a comprehensive understanding of access management needs by integrating geospatial road
39 inventory data, safety management data, land use planning information, and remote sensing data.
40 This holistic approach allows for more efficient and adequate decision-making in access manage-
41 ment projects.

42 Designing a research study that utilizes computer vision technology could be a unique
43 and valuable contribution to access management. By leveraging computer vision algorithms and
44 image processing techniques, it aims to develop a novel method to detect and count access points
45 along roadways automatically. This process can streamline the data collection, eliminating the

1 labor-intensive manual counting of driveways. By integrating computer vision with geospatial
2 road inventory data and land use planning information through GIS, a comprehensive and strategic
3 approach to access management can be achieved by this method. This study also performed the
4 accuracy and reliability of the applied algorithm in identifying different types of access points,
5 such as central residential, minor residential, major industrial, and others.

6 The rest of the paper is organized as follows. The Related Work section explores the litera-
7 ture review. The Methodology section provides a detailed presentation of the proposed framework.
8 The Experimental Analysis section outlines the dataset used for conducting experiments. The Re-
9 sults section presents the outcomes of the experiments and discusses the insights gained. Lastly,
10 the Conclusion section offers conclusions, highlights unique contributions, addresses limitations,
11 and suggests future research directions.

12 RELATED WORK

13 Urban road classification is a crucial task in transportation planning and management. Accurate
14 road classification helps authorities design efficient traffic management strategies, prioritize road
15 maintenance, and improve overall urban mobility. Our proposed framework focuses on the classi-
16 fication of urban roads from Remote Sensing Images (RSIs) based on the surrounding land use of
17 Point Of Interests (POIs).

18 The datasets used for land cover and land use classification exhibit variations in their cat-
19 egories, and efforts have been made to enhance surface coverage. Castillo-Navarro et al. (13)
20 have developed datasets covering multiple scenes to achieve this goal. However, these datasets
21 also differ in the labels attached to them (14). For example, SEN12MS (15) provides pixel-level
22 labels, while BigEarthNet [sumbul2019bigearthnet] offers image-level labels. Consequently, these
23 datasets are suitable for specific semantic segmentation applications due to their different scene
24 categories.

25 In the context of land use and land cover (LULC) classification, numerous semantic classes
26 exist, including hundreds of fine-grained classes such as buildings, roads, vehicles, countryside,
27 and urban areas. However, many existing datasets overlook the relationships within and between
28 semantic classes, neglecting important contextual information (16). High-resolution remote sens-
29 ing images (RSIs) provide rich and detailed spatial, geometric, and textural information (17), mak-
30 ing them ideal for accurate land-use classification. Over time, the development of land-use clas-
31 sification in RSIs has progressed from pixel-based image analysis to object-based image analysis
32 and pixel-level semantic segmentation (18).

33 Traditional classification methods have mainly relied on spectral information from low-
34 resolution remote sensing images, leading to suboptimal results for complex land-use types like
35 residential land and wasteland. The lack of comprehensive textural and structural features in
36 spectral features often hinders the accurate representation of land-use characteristics (19). To ad-
37 dress these limitations and improve the efficiency of training datasets, various techniques such
38 as Transfer Learning, Active Learning, and others have been developed (20). Researchers have
39 also explored pretraining networks for feature extraction, data domain adaptation, and migration
40 experiments to enhance classification accuracy (21, 22).

41 Object-oriented classification methods have emerged as a solution to the shortcomings of
42 pixel-based approaches. These methods consider the correlation between pixels and the internal
43 texture features of ground objects while utilizing spectral information from RSIs (23, 24). How-
44 ever, feature descriptions in these methods may still be inadequate to support precise classification

1 and recognition of ground objects.

2 Deep learning has revolutionized land-use classification in RSIs by capturing shape and
3 texture features of different objects, overcoming the limitations of traditional artificial features and
4 enabling pixel-level classification (25). Various deep learning models and hybrid frameworks have
5 been proposed, showing promising results in land-use scene classification and detailed mapping of
6 urban landscapes (26–28). Early FCN-based models could partially identify features but struggled
7 with issues such as loss of high-frequency details, blurred boundaries, and limited spatial informa-
8 tion reconstruction. To address these problems, a skip connection was incorporated into the net-
9 works. The U-Net Architecture, introduced by Ronneberger et al., employed a decoder structure
10 to aggregate multi-layer feature maps from the encoder through step-by-step upsampling, result-
11 ing in high-resolution feature maps (29). This fusion of high and low-level semantic information
12 enhanced the classification accuracy, especially for object boundaries.

13 In subsequent advancements, Yu and Koltun introduced atrous convolution into fully con-
14 volutional networks (FCN), allowing for the preservation of image resolution while expanding the
15 receptive field to capture multi-scale context information, thus improving semantic segmentation
16 accuracy using spatial information (30). To capture global context information more effectively,
17 Spatial Pyramid Pooling (SPP) (31) gained widespread adoption. Zhao et al. utilized a pyra-
18 mid pooling module to aggregate context from different regions, thereby leveraging the power of
19 global context information (32). Further innovations were made by Chen et al., who implemented
20 pyramid-shaped atrous pooling in spatial dimensions (33) and employed cascaded or parallel atrous
21 convolution (34) to gather multi-scale information (35). Despite the progress made with Atrous
22 Spatial Pyramid Pooling (ASPP) (33), limitations persisted, as the resolution in the scale axis di-
23 mension was insufficient to accurately extract target features in remote sensing images (RSIs).
24 To overcome these limitations, Yang et al. proposed the densely-connected Atrous Spatial Pyra-
25 mid Pooling (DenseASPP) (36), which achieved a wider scale of the feature map and obtained
26 more comprehensive receptive field information. This allowed for better classification of complex
27 scenes without increasing the model size. In addition, crowdsourced data, such as points of inter-
28 est (POIs), has also been applied for classification, offering an alternative to current methodologies
29 for LULC classification (37). Linked open geospatial data, including POI data, has shown poten-
30 tial as inputs for land-use classification models (38). Combined deep learning models have been
31 developed to tackle the challenge of limited well-annotated samples. For example, Semi-MCNN
32 selects and generates datasets from large amounts of unlabeled data, integrated with a multi-CNN
33 framework, to improve generalization ability and classification accuracy (39). For heterogeneous
34 urban land-cover, Zhang et al. proposed impervious surface area-weighted building-based indices
35 from building outline data, considering the varying contributions of different ground objects in
36 land-use classification, such as landscape patterns and building functions (40). These innovative
37 approaches and data sources contribute to advancing the field of land-use classification in remote
38 sensing images.

39 The literature review suggests a potential research need that involves exploring efficient
40 methods to integrate and utilize diverse data sources, including POIs, linked open geospatial data,
41 and crowdsourced data, to improve the accuracy of land-use classification and feature count related
42 data. This study aims to mitigate the research gap by enhancing the robustness and generalizability
43 of deep learning models, particularly when dealing with complex land-use types in regions with
44 diverse urban landscapes.

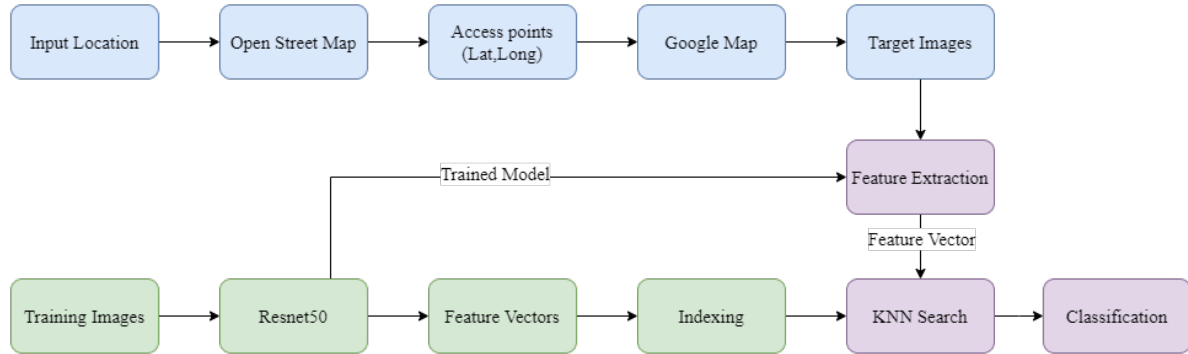


FIGURE 1 Proposed framework employs access point coordinates from Open Street Map, access point satellite images from Google Map, feature vectors from Resnet50, and k-NN search for classification.

1 METHODOLOGY

2 This paper presents a comprehensive framework shown in FIGURE 1, aimed at detecting and
 3 classifying driveway density in a given location, such as a city, state, or country. The proposed
 4 framework leverages various data sources, including Open Street Map (OSM) road network data,
 5 Google Map satellite images, and the k-Nearest Neighbor (k-NN) search in deep features.

- 6 • The first step of the framework involves extracting the latitude and longitude coordinates
 7 of all available access points in the target location using the OSM road network data.
 8 These access points serve as reference points for further analysis.
- 9 • Next, a database of satellite images is created for each access point based on its latitude
 10 and longitude. This is accomplished by collecting satellite images from Google's satellite
 11 image collection. Each access point is associated with a relevant satellite image.
- 12 • To extract meaningful features from these satellite images, a pre-trained Deep Neural
 13 Network (DNN) model is utilized. Specifically, the Resnet-50 (41) model, trained on the
 14 NWPU-RESISC45 (42) and UC Merced Land-Use (43) datasets, is employed for feature
 15 extraction. This allows for the extraction of high-level representations of the satellite
 16 images.
- 17 • Once the deep features are obtained, a k-NN index is built using the feature vectors. The
 18 k-NN search is then performed on this index to retrieve similar items (in this case, the
 19 training images) for each access point. The user can adjust the parameter k, representing
 20 the number of nearest neighbors to consider.
- 21 • To determine the classification of each access point, a majority voting approach is applied
 22 to the retrieval results. The winning class, determined by the most frequently retrieved
 23 category from the k-NN search, is assigned to the respective access point.

24 Overall, this framework offers a systematic approach to detect and classify driveway den-
 25 sity by combining road network data, satellite images, and deep feature extraction with k-NN
 26 search. It provides a valuable tool for analyzing and understanding the distribution of access
 27 points within a given location. The framework consists of three significant steps: Satellite im-
 28 age acquisition, Feature extraction using Deep Neural Network, and K-Nearest Neighbor Search
 29 and classification.

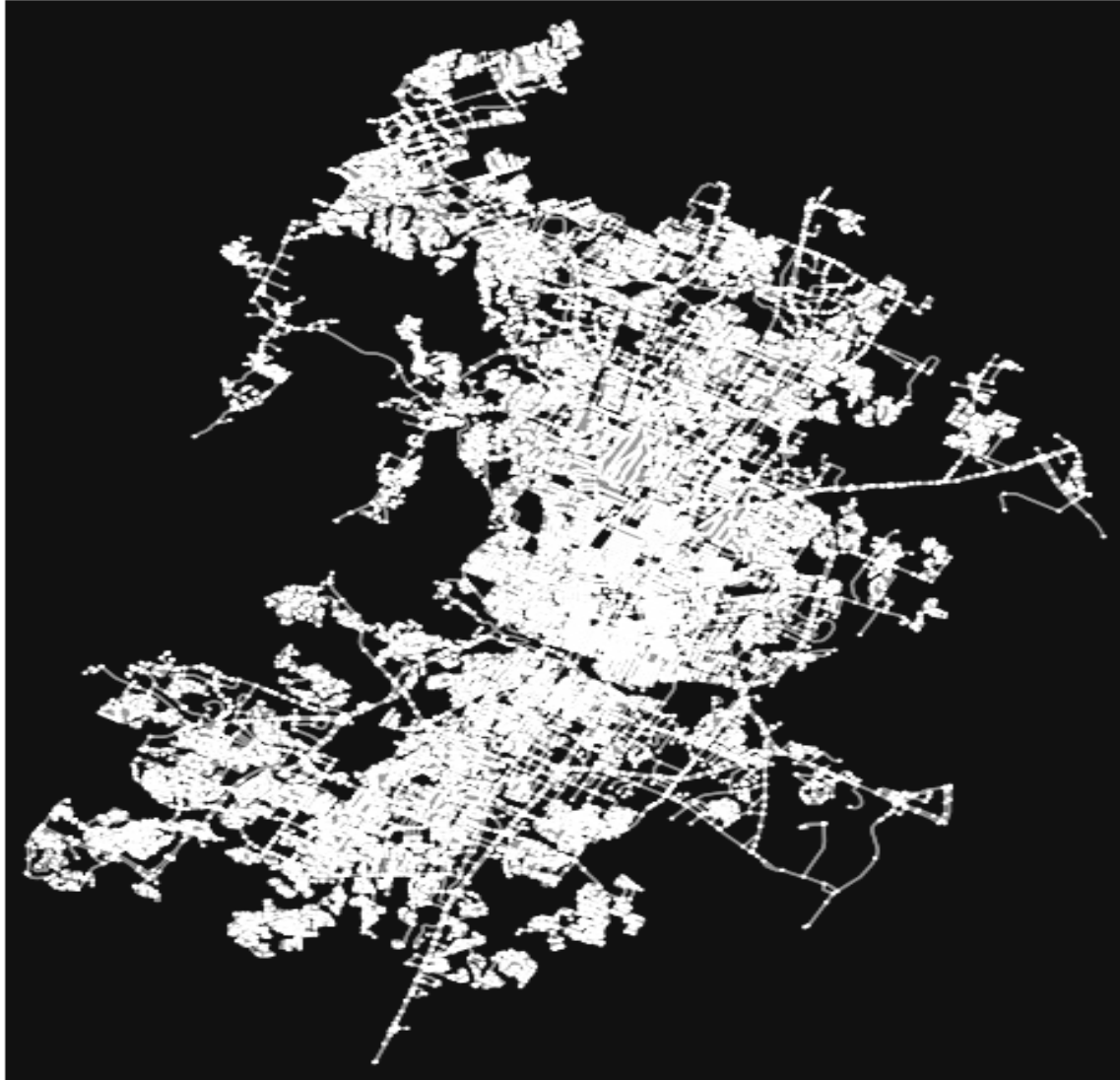


FIGURE 2 Road network for drivable urban roads for Austin, where nodes represent the access points and the edges represent the driveways.

1 **Satellite image acquisition**

2 The initial stage of our framework involves obtaining satellite images for the access points in a
3 specified target area. We utilized the OSMnx library, a Python package that retrieves, models,
4 analyzes, and visualizes street networks from Open Street Map. By employing OSMnx (44), we
5 extracted all the access points from the road network data. We focused on drivable urban access
6 points and obtained their corresponding geographic coordinates for our purposes.

7 FIGURE 2 shows the road network for driveable roads in Austin, where the nodes represent
8 the access points and the edges represent the driveways. Once we acquired the coordinates for these
9 access points, the next step was to download the respective satellite images from Google Maps.
10 We achieved this by utilizing a Python Client for Google Maps Services (45). By completing
11 these steps, we can create a comprehensive database of satellite images for access points in any

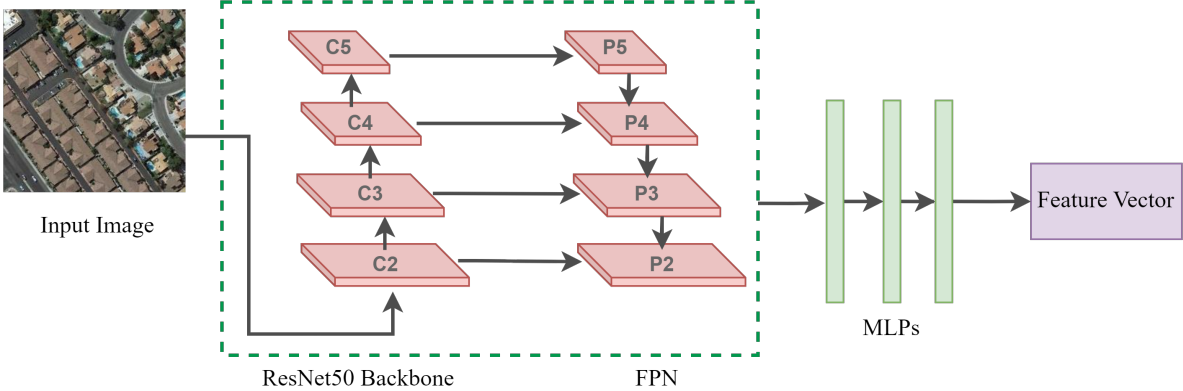


FIGURE 3 Feature extraction using Resnet50.

1 given location. Subsequently, we can classify these images as part of the subsequent stages in our
 2 framework.

3 Feature extraction using Deep Neural Network

4 The next step in driveway density classification involves efficient data representation. In our spe-
 5 cific case, the input data in our pipeline consists of images. Vector format is a widely used rep-
 6 resentation method for image data, and various approaches are available. One popular way is to
 7 use Deep Neural Networks (DNNs) to extract feature vectors. The success of DNNs in feature
 8 extraction can be attributed to factors such as the abundance of data and computational power.

9 Considering the previous achievements of DNNs in object detection within images (46–
 10 49), we have opted to employ the ResNet50 (41) architecture for generating feature vectors from
 11 our image data. FIGURE 3 illustrates that the ResNet50 model is constructed using multiple Con-
 12 volution (Conv) blocks stacked sequentially. The initial seven blocks in the ResNet50 network are
 13 Convolutional blocks with 64-channel outputs and a stride of one. The subsequent block begins
 14 with a Conv block having a stride of 2 and an output channel 128. This pattern continues with out-
 15 put channels 256 and 512. Following this, we apply average pooling to the output of the last Conv
 16 layer. Finally, we pass the result of the average pooling through Multi-layered Perceptrons (MLPs)
 17 and save the resulting output as a feature associated with its class in our database represented as
 18 a vector of length 2048. Later we use the deep feature database for k-Nearest Neighbor (k-NN)
 19 searching to retrieve similar images to a query image which we discuss later in detail.

20 In summary, for efficient driveway density classification, we first focus on representing
 21 the data efficiently. In the case of image data, we adopt the ResNet50 architecture, a popular
 22 DNN model, to extract feature vectors. These feature vectors are generated by passing the data
 23 through a series of Convolution blocks, followed by average pooling and MLPs, resulting in a
 24 vector representation of length 2048 associated with its class.

25 k-Nearest Neighbor (k-NN) Search and classification

26 After completing the previous steps in our framework, we proceed with the final stage, which
 27 involves conducting a k -NN search in the feature database using the pre-trained model. This search
 28 is performed against the target image, generating a 2048-dimensional feature vector for the target.
 29 We execute the k -NN search within our feature database for each of these target features, allowing

TABLE 1 Data set classes and distribution

Class name	Number of instances (Combined Train)	Number of instances (Austin Train)	Number of instances (Austin Test)
Major residential	1500	250	50
Minor residential	700	250	50
Major commercial	570	250	50
Minor commercial	70	250	50
Major industrial	475	250	50
Minor industrial	150	250	50

1 us to obtain the k most similar items. Next, we assign the winning class to label the target image
 2 by applying majority voting to the retrieved classes.

3 EXPERIMENTAL ANALYSIS

4 All experiments were carried out on Windows 10, 64-bit with Intel(R) Xeon(R) Gold 5217 CPU
 5 @ 3.0 GHz with 196GB RAM and NVIDIA GeForce RTX A5000 24GB mem GPU.

6 Training Dataset

7 To classify driveways into six target classes (Major residential, Minor residential, Major indus-
 8 trial, Minor industrial, Major commercial, and Major commercial), we encountered a challenge in
 9 finding a single data set containing all six classes. To address this issue, we decided to create a
 10 new data set by combining two existing data sets: the UC Merced Land Use (43) data set and the
 11 NWPU-RESISC45 (42) data set.

12 The UC Merced Land Use (43) data set originally consisted of 21 classes, each containing
 13 100 images. However, we selected only three classes from this data set for our driveway classifica-
 14 tion task: dense residential, medium residential, and sparse residential. These classes were chosen
 15 because they represented residential areas and were relevant to our classification problem. On the
 16 other hand, the NWPU-RESISC45 (42) data set contained 45 classes, with 700 images per class. In
 17 addition to the three residential classes from the UC Merced Land Use data set, we also included
 18 the commercial and industrial area classes from the NWPU-RESISC45 data set. These classes
 19 were included because they represented commercial and industrial areas, important categories for
 20 classifying driveways.

21 By combining these selected classes from the UC Merced Land Use data set and the
 22 NWPU-RESISC45 data set, we created a comprehensive data set that covered a broader range
 23 of classes related to driveways. This hybrid data set allowed us to train a classification model
 24 distinguishing between major and minor residential and industrial areas and primary and minor
 25 commercial areas. By leveraging relevant classes from multiple data sets, we aimed to increase
 26 the diversity and representatives of our training data, enabling our model to generalize better and
 27 accurately classify driveways into the desired target classes.

28 Next, we performed data pre-processing by combining the dense residential and medium
 29 residential classes from both data sets, which resulted in a new class called central residential.
 30 Similarly, we combined the sparse residential classes from both data sets into a minor residential
 31 class. This consolidation helped simplify the classification process. We visually separated the

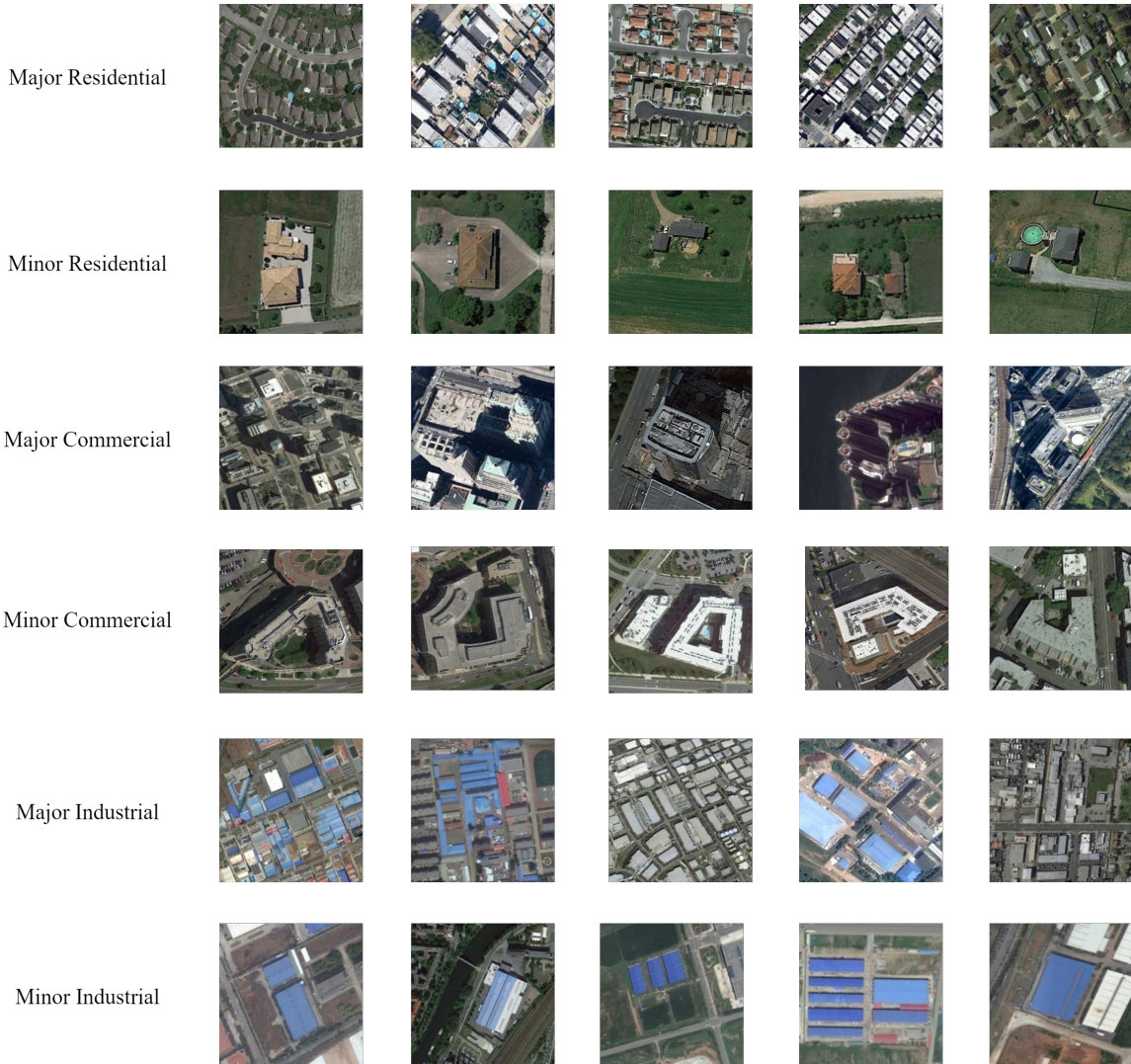


FIGURE 4 Sample combined training data set with six classes: Major residential, Minor residential, Major commercial, Minor commercial, Major industrial, and Minor industrial.

1 commercial area class images from the NWPU-RESISC45 data set into two sub-classes: major
 2 commercial and minor commercial. Likewise, we applied the same approach to the industrial area
 3 class, creating significant and insignificant industrial classes. By doing this, we aimed to refine the
 4 categorization and improve the clarity of the data. Some training samples from the hybrid data set
 5 are shown in FIGURE 4.

6 After these modifications, our final combined training data set consisted of six classes:
 7 central residential, minor residential, major commercial, minor commercial, major industrial, and
 8 minor industrial. To test the DNN model's applicability, we also built a test data set by manually
 9 annotating the satellite images from Google Maps for the city of Austin into the six classes above.
 10 However, after thoroughly examining the combined training data set and Austin test data set, we
 11 have found that the building design and pattern are quite different for the city of Austin than that
 12 of the combined training data. Therefore, we have built a more balanced training data set from the

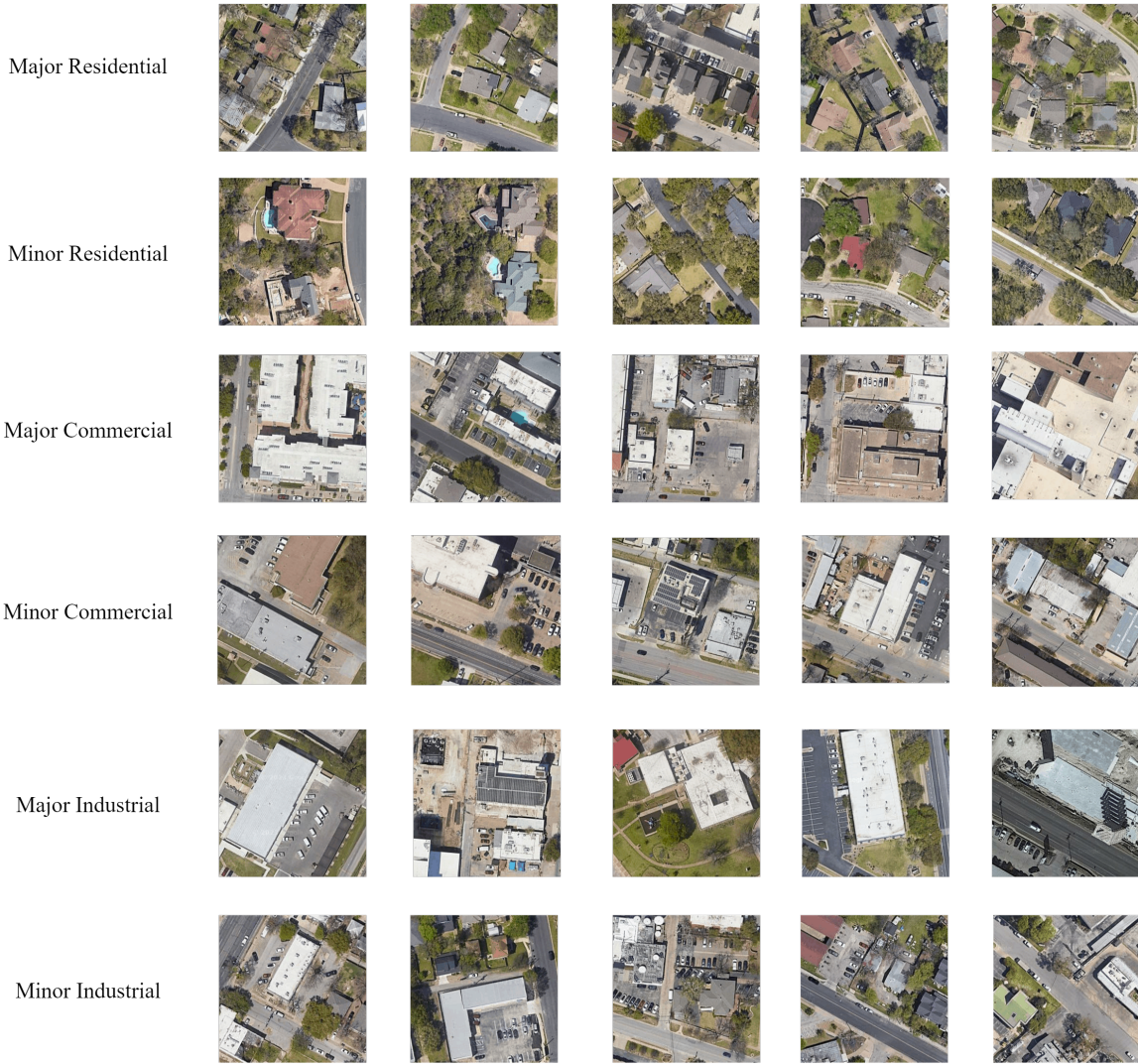


FIGURE 5 Sample Austin training data set with six classes: Major residential, Minor residential, Major commercial, Minor commercial, Major industrial, and Minor industrial.

1 satellite images from Google Maps for Austin. Some sample images from the Austin training data
 2 set are shown in FIGURE 5). The distribution of combined training, Austin training, and Austin
 3 test data set is presented in TABLE 1.

4 During our analysis of the training data set, we noticed a significant similarity between
 5 the samples belonging to major commercial and minor commercial and major industrial and little
 6 industrial classes. This high inter-class similarity posed a challenge for our Deep Neural Network
 7 (DNN) model, which frequently misclassified images from these similar class pairs. We have
 8 documented this issue in the Results Section. To address this problem, we incorporated a k -NN
 9 search technique into our classification pipeline. With the k -NN search, we retrieve the k most
 10 similar items from our feature database when presented with an input image. We then employ
 11 majority voting, assigning the class that appears most frequently among the retrieved similar things
 12 to the input image.

TABLE 2 Notation table.

Symbol	Description
TP	True positive
TN	True negative
FP	False positive
FN	False negative

Our rationale behind adopting the k -NN search and majority voting is to leverage the similarities between images in the feature database to enhance the accuracy of our classification process. By incorporating this approach, we aim to mitigate the misclassification issues caused by the high inter-class similarity between certain classes. Detailed results and further analysis can be found later in this section.

6 Performance metrics

We have used four metrics to measure the performance of the Deep Neural Network (DNN) model: accuracy, recall, Precision, and F1-score. All the notation symbol and their description in this section are shown in TABLE 2.

Accuracy measures the overall correctness of a classification model. It is calculated as the ratio of correctly predicted data instances to the total number of data instances in the data set. The formula for calculating accuracy is given in equation 1.

$$Accuracy = \frac{TP + TN}{TP + TN + FP + FN} \quad (1)$$

TABLE 3 Hyper-parameter settings for DNN train

Hyper-Parameter	Value
Batch-Size	32
Num. of Epoch	15
Loss Function	Cross-Entropy
Optimizer	Stochastic Gradient Descent (SGD)
Class in Dataset	6

Recall measures the ability of a classification model to correctly identify positive instances (e.g., true positives) out of all actual positive instances (e.g., true positives and false negatives). The formula for calculating accuracy is given in equation 2.

$$Recall = \frac{TP}{TP + FN} \quad (2)$$

Precision measures the accuracy of the positive predictions made by the model. It is calculated as the ratio of true positive instances to the total number of cases predicted as positive (true positives and false positives). The formula for calculating accuracy is given in equation 3.

$$Precision = \frac{TP}{TP + FP} \quad (3)$$

F1-score is the harmonic mean of precision and recall. It combines both metrics to provide a score that balances precision and recall. The formula for calculating accuracy is given in equation

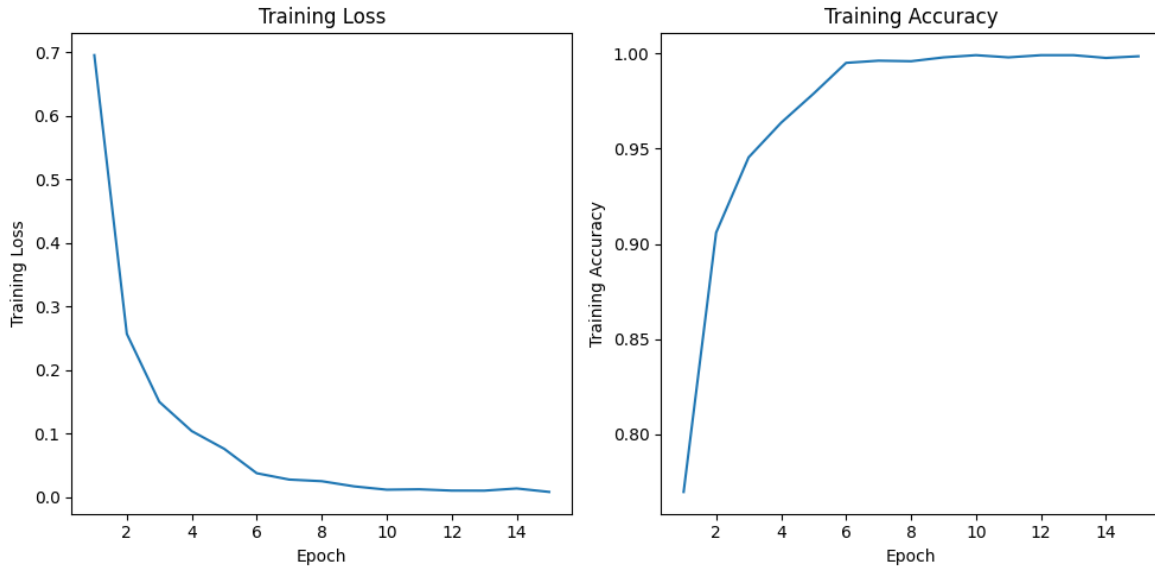


FIGURE 6 Train accuracy and loss on combined train data set w.r.t Number of epochs.

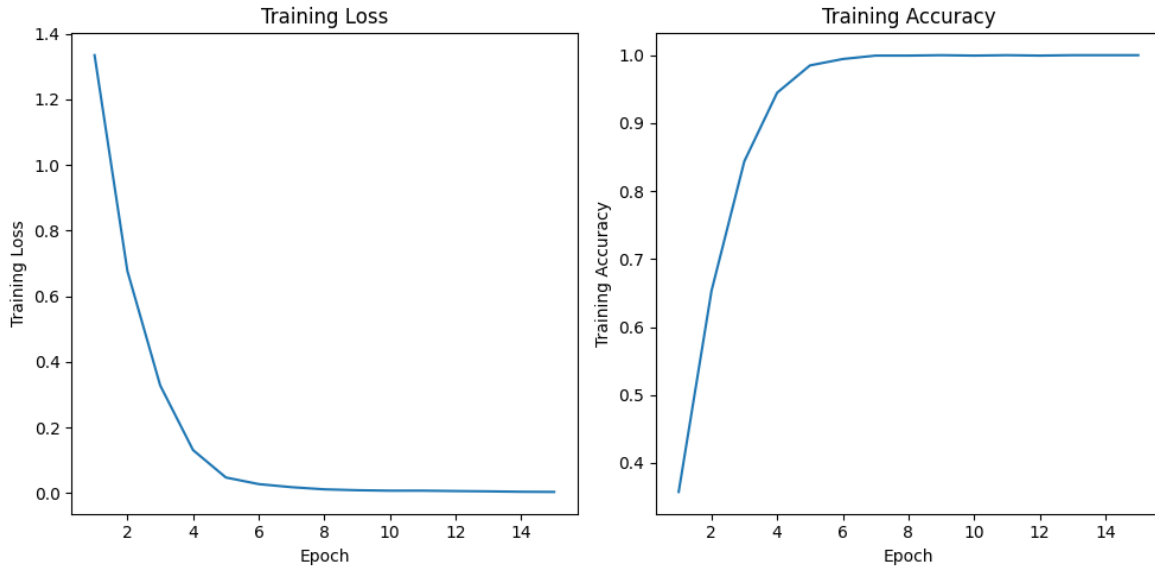


FIGURE 7 Train accuracy and loss on Austin train data set w.r.t Number of epochs.

1 4.

$$F1-score = 2 \times \frac{Precision \times Recall}{Precision + Recall} \quad (4)$$

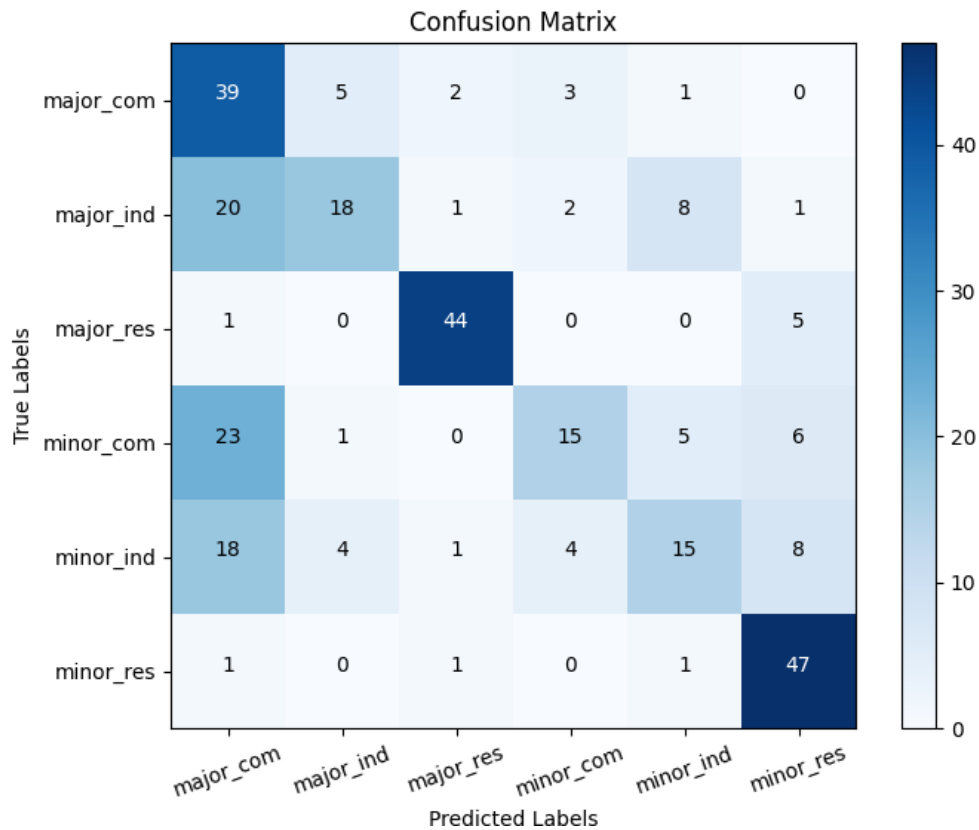
2 RESULTS

- 3 Our initial step in the feature DNN training process involved training the ResNet50 model using
4 the combined train data, following the specifications provided in TABLE 3. The performance of

TABLE 4 Hyper-parameter settings for DNN train

Metric	Resnet50 trained on combined data set		Resnet50 trained on Austin data set	
	without k -NN search	with k -NN search	without k -NN search	with k -NN search
Accuracy	42.75%	43.79%	61.00%	59.33%
Recall	21.56%	21.63%	61.00%	59.33%
Precision	17.68%	24.74%	60.50%	62.49%
F1-score	19.43%	23.08%	60.75%	60.87%

- 1 the ResNet50 model during the training phase was impressive, yielding a high training accuracy
 2 of 99.83%. The accuracy and loss trends of the model during training are visualized in Figure 6,
 3 demonstrating its proficiency in learning from the training data.

**FIGURE 8 Confusion matrix for the classification with k -NN search of the Austin satellite image data set.**

- 4 However, its performance was disappointing when we tested the trained model on the
 5 Austin test image dataset. The model achieved an accuracy of only 42.75% on the Austin satel-
 6 lite image data set (as shown in TABLE 4). The recall, precision, and f1-score for the Austin
 7 test dataset were also relatively low, indicating poor performance in correctly identifying positive
 8 instances.

1 To address this issue, we took a different approach. We retrained the model using only the
2 Austin train dataset while keeping the hyper-parameters the same as those in TABLE 3. Surpris-
3 ingly, the model’s performance significantly improved during this second training phase, achieving
4 an accuracy of 99.94% (as shown in FIGURE 7). When tested on the Austin test dataset, the model
5 achieved an accuracy of 61%, showcasing an impressive 18.75% improvement in accuracy com-
6 pared to training on the combined train dataset. Furthermore, the recall, precision, and f1-score
7 also exhibited noticeable improvements over the previous approach (as summarized in TABLE 4).

8 We employed the *k*-NN search technique to further enhance classification performance by
9 extracting deep features during the training phase. As demonstrated in TABLE 4, the *k*-NN search
10 contributed to improved classification performance compared to using only the ResNet50 model
11 for each comparison metric. Nevertheless, the improvement was limited due to the challenges
12 posed by the dataset’s imbalance and high inter-class similarity. The confusion matrix presented in
13 FIGURE 8 revealed that the classification with the *k*-NN search often confused between major and
14 minor classes, mainly because of the similarities between corresponding major and minor classes.

15 The results indicate that training the model specifically on the Austin train data set led to
16 substantial performance improvements. However, despite using the *k*-NN search, challenges aris-
17 ing from high inter-class similarity remain limiting factors in achieving further significant improve-
18 ments in classification accuracy. Addressing these challenges and exploring additional techniques
19 may be essential for enhancing the overall classification performance and ensuring more accurate
20 and robust results.

21 CONCLUSION AND FUTURE WORK

22 In conclusion, this paper sheds light on the dual role of roadways in facilitating driver mobility
23 and providing access to land development and commercial establishments. The coexistence of
24 high-speed traffic and direct entry points to properties often leads to conflicts, necessitating effec-
25 tive access management strategies. The careful planning and control of entry points to arterial and
26 collector roadway systems become essential in addressing these challenges. Access points play a
27 crucial role in connecting public roadways with adjacent properties, but they also pose significant
28 risks, contributing to traffic accidents and congestion. Therefore, it is imperative to focus on ac-
29 cess management initiatives to mitigate these adverse effects. While traditional approaches often
30 concentrate on specific corridors, this paper introduces a more strategic approach by leveraging
31 geographic information systems (GIS) to enhance overall efficiency and decision-making.

32 The comprehensive framework proposed in this paper offers a promising solution for de-
33 tecting and classifying driveway density in a given location. The framework identifies access point
34 coordinates using Open Street Map (OSM) road network data and Google Map satellite images. It
35 applies a pre-trained Deep Neural Network (DNN) model to extract deep features. The subsequent
36 application of the k-Nearest Neighbor (*k*-NN) search results in an f1-score of 60.87%, outperform-
37 ing the conventional DNN model by 0.12%, as demonstrated on the experimental Austin satel-
38 lite image data. This framework’s success indicates its potential to enhance access management
39 strategies and improve road safety in various locations. By harnessing advanced technologies and
40 geospatial data, the framework offers a promising avenue to address access-related challenges and
41 promote efficient and safe transportation systems. The framework developed in this paper will be
42 beneficial in populating the needed driveway density information for the urban/rural roadway SPF
43 development.

44 Several limitations of the current study should be acknowledged, including the dependence

1 on dataset size and quality, potential inaccuracies in driveway classification, and computational
2 complexity. In future research, expanding the dataset to improve generalizability, implementing
3 real-time solutions for practical application, integrating the framework with traffic management
4 systems, and addressing privacy concerns are essential areas of focus. Evaluating the long-term
5 impact of access management strategies based on the framework's recommendations is also cru-
6 cial to measure effectiveness in improving road safety and traffic flow. Despite these limitations,
7 the framework offers a promising avenue for addressing access-related challenges and promoting
8 efficient and safe transportation systems.

9 **ACKNOWLEDGMENT**

10 The authors thank Catalina Gonzalez and Khaled Aly Abousabaa for their tremendous assistance
11 annotating driveway types.

12 **AUTHORSHIP CONTRIBUTION STATEMENT**

13 The authors confirm their contribution to the paper as follows: study conception and design: S.
14 Das, M. Rahman; data collection: S. Das, M. Rahman; analysis and interpretation of results: M.
15 Rahman, S. Das, J. Tešić; draft manuscript preparation: M. Rahman, S. Das, J. Tešić; All authors
16 reviewed the results and approved the final version of the manuscript.

17 **DECLARATION OF CONFLICTING INTEREST**

18 The author(s) declared no potential conflicts of interest concerning this article's research, author-
19 ship, and/or publication.

20 **REFERENCES**

- 21 1. Souleyrette, R. R., P. Plazak, and D. J. Plazak, Use of geospatial information and remote
22 sensing data to support improved roadway access management. *WIT Transactions on The
23 Built Environment*, Vol. 89, 2006.
- 24 2. Gluck, J., H. S. Levinson, and V. Stover, Impacts of Access Management Techniques,
25 NCHRP Report 420. *Transportation Research Board*, 1999.
- 26 3. Williamson, M. and H. Zhou, A study of safety impacts of different types of driveways
27 and their density. *Procedia-social and behavioral sciences*, Vol. 138, 2014, pp. 576–583.
- 28 4. Vaiana, R., G. Perri, T. Iuele, and V. Gallelli, A comprehensive approach combining reg-
29 ulatory procedures and accident data analysis for road safety management based on the
30 European Directive 2019/1936/EC. *Safety*, Vol. 7, No. 1, 2021, p. 6.
- 31 5. Gattis, J., *Guide for the geometric design of driveways*, Vol. 659. Transportation Research
32 Board, 2010.
- 33 6. Azzeh, J. A., B. A. Thorson, J. J. Valenta, J. C. Glennon, and C. Wilton, *Evaluation of
34 techniques for the control of direct access to arterial highways*, 1975.
- 35 7. Levinson, H. S., J. S. Gluck, J. M. Barlow, R. W. Eck, and W. F. Hecker, Driveway design
36 practices, issues, and needs. In *3rd Urban Street Symposium: Uptown, Downtown, or
37 Small Town: Designing Urban Streets That Work* *Transportation Research Board Institute
38 of Transportation Engineers (ITE) US Access Board*, 2007.
- 39 8. McLean, J., *Practical Relationships for the Assessment of Road Feature Treatments: Sum-
40 mary Report*. ARR 315, 1997.

- 1 9. Chakraborty, M. and T. J. Gates, Association between driveway land use and safety performance on rural highways. *Transportation research record*, Vol. 2675, No. 1, 2021, pp. 114–124.
- 2 10. Levinson, H. S., Access Spacing and Accidents. In *Urban Street Symposium*, 1999.
- 3 11. on Development of the Highway Safety Manual, N. R. C. U. T. R. B. T. F., A. A. of State Highway, T. O. J. T. F. on the Highway Safety Manual, and N. C. H. R. Program, *Highway Safety Manual*. No. v. 1 in Highway Safety Manual, American Association of State Highway and Transportation Officials, 2010.
- 4 12. Associates, K. ., U. S. F. T. Administration, T. C. R. Program, and T. D. Corporation, *Transit capacity and quality of service manual*, Vol. 42. Transportation Research Board, 2003.
- 5 13. Castillo-Navarro, J., B. Le Saux, A. Boulch, N. Audebert, and S. Lefèvre, Semi-Supervised Semantic Segmentation in Earth Observation: The MiniFrance suite, dataset analysis and multi-task network study. *Machine Learning*, 2021, pp. 1–36.
- 6 14. Wilhelm, T. and D. Koßmann, Land cover classification from a mapping perspective: Pixelwise supervision in the deep learning era. In *2021 IEEE International Geoscience and Remote Sensing Symposium IGARSS*, IEEE, 2021, pp. 2496–2499.
- 7 15. Schmitt, M., L. H. Hughes, C. Qiu, and X. X. Zhu, SEN12MS—A Curated Dataset of Georeferenced Multi-Spectral Sentinel-1/2 Imagery for Deep Learning and Data Fusion. *arXiv preprint arXiv:1906.07789*, 2019.
- 8 16. Long, Y., G.-S. Xia, S. Li, W. Yang, M. Y. Yang, X. X. Zhu, L. Zhang, and D. Li, On creating benchmark dataset for aerial image interpretation: Reviews, guidances, and million-aid. *IEEE Journal of selected topics in applied earth observations and remote sensing*, Vol. 14, 2021, pp. 4205–4230.
- 9 17. Richards, J. A., J. A. Richards, et al., *Remote sensing digital image analysis*, Vol. 5. Springer, 2022.
- 10 18. Neupane, B., T. Horanont, and J. Aryal, Deep learning-based semantic segmentation of urban features in satellite images: A review and meta-analysis. *Remote Sensing*, Vol. 13, No. 4, 2021, p. 808.
- 11 19. Pan, X. and J. Zhao, High-resolution remote sensing image classification method based on convolutional neural network and restricted conditional random field. *Remote Sensing*, Vol. 10, No. 6, 2018, p. 920.
- 12 20. Ma, L., Y. Liu, X. Zhang, Y. Ye, G. Yin, and B. A. Johnson, Deep learning in remote sensing applications: A meta-analysis and review. *ISPRS journal of photogrammetry and remote sensing*, Vol. 152, 2019, pp. 166–177.
- 13 21. Ammour, N., L. Bashmal, Y. Bazi, M. M. Al Rahhal, and M. Zuair, Asymmetric adaptation of deep features for cross-domain classification in remote sensing imagery. *IEEE Geoscience and Remote Sensing Letters*, Vol. 15, No. 4, 2018, pp. 597–601.
- 14 22. Zhou, X. and S. Prasad, Deep feature alignment neural networks for domain adaptation of hyperspectral data. *IEEE Transactions on Geoscience and Remote Sensing*, Vol. 56, No. 10, 2018, pp. 5863–5872.
- 15 23. Walter, V., Object-based classification of remote sensing data for change detection. *ISPRS Journal of photogrammetry and remote sensing*, Vol. 58, No. 3-4, 2004, pp. 225–238.

- 1 24. Chen, W., X. Li, H. He, and L. Wang, A review of fine-scale land use and land cover clas-
2 sification in open-pit mining areas by remote sensing techniques. *Remote Sensing*, Vol. 10,
3 No. 1, 2017, p. 15.
- 4 25. Wu, H., B. Liu, W. Su, W. Zhang, and J. Sun, Deep filter banks for land-use scene classi-
5 fication. *IEEE Geoscience and Remote Sensing Letters*, Vol. 13, No. 12, 2016, pp. 1895–
6 1899.
- 7 26. Xu, S., S. Zhang, J. Zeng, T. Li, Q. Guo, and S. Jin, A framework for land use scenes
8 classification based on landscape photos. *IEEE Journal of Selected Topics in Applied Earth
9 Observations and Remote Sensing*, Vol. 13, 2020, pp. 6124–6141.
- 10 27. Gibril, M. B. A., B. Kalantar, R. Al-Ruzouq, N. Ueda, V. Saeidi, A. Shanableh, S. Mansor,
11 and H. Z. Shafri, Mapping heterogeneous urban landscapes from the fusion of digital
12 surface model and unmanned aerial vehicle-based images using adaptive multiscale image
13 segmentation and classification. *Remote Sensing*, Vol. 12, No. 7, 2020, p. 1081.
- 14 28. Zhu, Y., C. Geiß, E. So, and Y. Jin, Multitemporal relearning with convolutional LSTM
15 models for land use classification. *IEEE Journal of Selected Topics in Applied Earth Ob-
16 servations and Remote Sensing*, Vol. 14, 2021, pp. 3251–3265.
- 17 29. Ronneberger, O., P. Fischer, and T. Brox, U-net: Convolutional networks for biomedical
18 image segmentation. In *Medical Image Computing and Computer-Assisted Intervention–
19 MICCAI 2015: 18th International Conference, Munich, Germany, October 5–9, 2015,
20 Proceedings, Part III 18*, Springer, 2015, pp. 234–241.
- 21 30. Yu, F. and V. Koltun, Multi-scale context aggregation by dilated convolutions. *arXiv
22 preprint arXiv:1511.07122*, 2015.
- 23 31. He, K., X. Zhang, S. Ren, and J. Sun, Spatial pyramid pooling in deep convolutional
24 networks for visual recognition. *IEEE transactions on pattern analysis and machine intel-
25 ligence*, Vol. 37, No. 9, 2015, pp. 1904–1916.
- 26 32. Zhao, H., J. Shi, X. Qi, X. Wang, and J. Jia, Pyramid scene parsing network. In *Pro-
27 ceedings of the IEEE conference on computer vision and pattern recognition*, 2017, pp.
28 2881–2890.
- 29 33. Chen, L.-C., G. Papandreou, I. Kokkinos, K. Murphy, and A. L. Yuille, Deeplab: Semantic
30 image segmentation with deep convolutional nets, atrous convolution, and fully connected
31 crfs. *IEEE transactions on pattern analysis and machine intelligence*, Vol. 40, No. 4, 2017,
32 pp. 834–848.
- 33 34. Chen, L.-C., G. Papandreou, F. Schroff, and H. Adam, Rethinking atrous convolution for
34 semantic image segmentation. *arXiv preprint arXiv:1706.05587*, 2017.
- 35 35. Chen, L.-C., Y. Zhu, G. Papandreou, F. Schroff, and H. Adam, Encoder-decoder with
36 atrous separable convolution for semantic image segmentation. In *Proceedings of the Eu-
37 ropean conference on computer vision (ECCV)*, 2018, pp. 801–818.
- 38 36. Yang, M., K. Yu, C. Zhang, Z. Li, and K. Yang, Denseaspp for semantic segmentation
39 in street scenes. In *Proceedings of the IEEE conference on computer vision and pattern
40 recognition*, 2018, pp. 3684–3692.
- 41 37. Andrade, R., A. Alves, and C. Bento, POI mining for land use classification: A case study.
42 *ISPRS International Journal of Geo-Information*, Vol. 9, No. 9, 2020, p. 493.
- 43 38. Re Calegari, G., E. Carlino, D. Peroni, and I. Celino, Extracting urban land use from linked
44 open geospatial data. *ISPRS International Journal of Geo-Information*, Vol. 4, No. 4, 2015,
45 pp. 2109–2130.

- 1 39. Fan, R., R. Feng, L. Wang, J. Yan, and X. Zhang, Semi-MCNN: A semisupervised multi-
2 CNN ensemble learning method for urban land cover classification using submeter HRSS
3 images. *IEEE Journal of Selected Topics in Applied Earth Observations and Remote Sensing*, Vol. 13, 2020, pp. 4973–4987.
- 4 40. Zhang, Y., K. Qin, Q. Bi, W. Cui, and G. Li, Landscape patterns and building functions for
5 urban land-use classification from remote sensing images at the block level: a case study
6 of Wuchang District, Wuhan, China. *Remote Sensing*, Vol. 12, No. 11, 2020, p. 1831.
- 7 41. He, K., X. Zhang, S. Ren, and J. Sun, Deep residual learning for image recognition. In
8 *Proceedings of the IEEE conference on computer vision and pattern recognition*, 2016,
9 pp. 770–778.
- 10 42. Cheng, G., J. Han, and X. Lu, Remote Sensing Image Scene Classification: Benchmark
11 and State of the Art. *Proceedings of the IEEE*, Vol. 105, No. 10, 2017, pp. 1865–1883.
- 12 43. Yang, Y. and S. Newsam, Bag-Of-Visual-Words and Spatial Extensions for Land-Use Clas-
13 sification. In *ACM SIGSPATIAL International Conference on Advances in Geographic In-*
14 *formation Systems (ACM GIS)*, 2010.
- 15 44. Boeing, G., OSMnx: New methods for acquiring, constructing, analyzing, and visualizing
16 complex street networks. *Computers, Environment and Urban Systems*, Vol. 65, 2017, pp.
17 126–139.
- 18 45. Google, *Google Maps Python Client*. <https://github.com/googlemaps/google-maps-services-python>, 2023, accessed: July 13, 2023.
- 19 46. Biswas, D., M. M. M. Rahman, Z. Zong, and J. Tešić, Improving the Energy Efficiency
20 of Real-time DNN Object Detection via Compression, Transfer Learning, and Scale Pre-
21 diction. In *2022 IEEE International Conference on Networking, Architecture and Storage*
22 (*NAS*), 2022, pp. 1–8.
- 23 47. Albaba, B. M. and S. Ozer, SyNet: An ensemble network for object detection in UAV im-
24 ages. In *2020 25th International Conference on Pattern Recognition (ICPR)*, IEEE, 2021,
25 pp. 10227–10234.
- 26 48. Zhu, X., S. Lyu, X. Wang, and Q. Zhao, TPH-YOLOv5: Improved YOLOv5 based on
27 transformer prediction head for object detection on drone-captured scenarios. In *Pro-
28 ceedings of the IEEE/CVF international conference on computer vision*, 2021, pp. 2778–2788.
- 29 49. Redmon, J. and A. Farhadi, YOLO9000: Better, Faster, Stronger. *CoRR*, Vol.
30 abs/1612.08242, 2016.